

Anharmonicity and cross section for absorption of radiation by water dimer

H. C. W. Tso, D. J. W. Geldart, and Petr Chýlek

Citation: *The Journal of Chemical Physics* **108**, 5319 (1998); doi: 10.1063/1.475967

View online: <http://dx.doi.org/10.1063/1.475967>

View Table of Contents: <http://scitation.aip.org/content/aip/journal/jcp/108/13?ver=pdfcov>

Published by the [AIP Publishing](#)

Articles you may be interested in

[Vibrational absorption and vibrational circular dichroism spectra of leucine in water under different pH conditions: Hydrogen-bonding interactions with water](#)

J. Chem. Phys. **137**, 194308 (2012); 10.1063/1.4767401

[Communication: Spectroscopic measurement of the binding energy of a carboxylic acid-water dimer](#)

J. Chem. Phys. **136**, 171101 (2012); 10.1063/1.4711862

[Multimode simulation of dimer absorption spectra from first principles calculations: Application to the 3,4,9,10-perylenetetracarboxylic diimide dimer](#)

J. Chem. Phys. **131**, 154302 (2009); 10.1063/1.3245403

[Anharmonic midinfrared vibrational spectra of benzoic acid monomer and dimer](#)

J. Chem. Phys. **123**, 014305 (2005); 10.1063/1.1947191

[High-resolution ultraviolet spectroscopy of p -fluorostyrene-water: Evidence for a \$\sigma\$ -type hydrogen-bonded dimer](#)

J. Chem. Phys. **122**, 244312 (2005); 10.1063/1.1937370



NEW Special Topic Sections

NOW ONLINE
Lithium Niobate Properties and Applications:
Reviews of Emerging Trends

AIP | Applied Physics
Reviews

Anharmonicity and cross section for absorption of radiation by water dimer

H. C. W. Tso, D. J. W. Geldart, and Petr Chýlek

Department of Physics, Dalhousie University, Halifax, Nova Scotia, Canada B3H 3J5

(Received 26 November 1997; accepted 24 December 1997)

We calculate the absorption cross section of water dimer molecules in thermal equilibrium at temperatures typical of the lower atmosphere using quantum mechanical coupled nonlinear equations of motion. Empirical Morse-oscillator potentials are used to describe the local modes of water monomer, and the RWK2 potential is employed for the interaction between atoms of different water monomers. The strong anharmonicity is taken into account by an extension to molecular dimers of methods originally developed for the lattice dynamics of solid helium. Approximations based on exploiting the hierarchy of energy scales in the dynamics of the weakly hydrogen-bonded water dimer allow the determination of the absorption spectrum over the range of significant solar radiation, up to $20\,000\text{ cm}^{-1}$, including the important contributions of overtone and combination transitions. This approach can tackle the complicated task of mixing of vibrational fundamentals and overtones. We have found that the absorption by these vibrational overtones, within the solar energy range, is quite significant due to the anharmonicity of Morse-oscillator potentials and the large vibrational amplitude of hydrogen atoms. These overtones may play a role in the solar energy absorption of the atmosphere. © 1998 American Institute of Physics. [S0021-9606(98)01613-4]

I. INTRODUCTION

Water vapor in the atmosphere is a strong absorber of solar radiation. Experimental studies of the absorption of solar radiation in the earth's atmosphere have suggested that under cloudy sky conditions, the atmosphere absorbs 25 to 30 W/m^2 more of the incoming solar radiation than is accounted for by currently accepted theoretical models.¹⁻⁴ Some excess absorption has also been reported under clear sky conditions.^{5,6} It is not clear whether the excess absorption is specifically due to clouds or is correlated with the total water vapor concentration.⁷ The reported excess absorption amounts to a difference of more than 25% in the model predictions of atmospheric absorption, or about 8% of the total incoming solar radiation at the top of the atmosphere. A discrepancy of this magnitude would have significant implications for global climate models, including predictions of global change and related current environmental issues.⁸⁻¹⁰

Current models consider all water vapor be in the form of water monomers. However, a fraction of the total water content will be present in the form of water dimers, which are weakly hydrogen-bonded $(\text{H}_2\text{O})_2$ molecules. Thermodynamic arguments yield estimates of the ratio of dimer to monomer concentrations, c_D/c_M of order 10^{-3} , assuming local thermal equilibrium at the relevant temperature and relative humidity. Recent studies^{11,12} suggest that water vapor dimer may contribute to the solar energy absorption of the atmosphere. Although the vibrational spectroscopy of water dimer has been studied extensively both theoretically¹³⁻²¹ and experimentally,²¹⁻²⁸ all of these studies focused on frequencies below 4000 cm^{-1} . On the other hand, the solar spectrum has frequencies far beyond 4000 cm^{-1} . In view of this, it is necessary to determine the intrinsic absorp-

tion cross section for dimer molecules, $\sigma_D(\omega)$, as a function of frequency (ω).

In this paper, we study the absorption cross section of water dimers up to $20\,000\text{ cm}^{-1}$ at a temperature of $10\text{ }^\circ\text{C}$. We adopt the RWK2 model^{17,19} potential Φ for the interaction between donor and acceptor molecules. This interaction leads to an intermolecular absorption band with wave numbers up to 800 cm^{-1} . On the other hand, the intramolecular vibrational spectrum of the water molecule due to the stretching and bending motions of the O-H bonds has narrow absorption bands at about 1500 and 3600 cm^{-1} . Due to the weakness of the hydrogen bond and the small mass of hydrogen atoms, relative displacements of individual nuclei from their equilibrium positions can be large. Consequently, anharmonicity of the potential energy surface becomes important and absorption due to overtones of these excitations is significant.

Before giving an outline of the calculations, we indicate the general rationale for our approximations. First, we make the usual Born-Oppenheimer approximation. This is a generic approximation for such molecular problems and amounts to decoupling the fast electron dynamics from the slow nuclear motion. The expansion parameter for the energy in this approximation is the square root of the electron to ion mass ratio, which is of order 0.02 for the hydrogen mass. The second expansion parameter is specific to a weakly hydrogen-bonded molecule. The ratio of the dimer to monomer binding energy is about 0.05. Thus the ratio of the average intermolecular frequency to the average intramolecular frequency squared, $\bar{\omega}_{\text{inter}}^2/\bar{\omega}_{\text{intra}}^2$, is about 0.01. This implies that the intermolecular and the intramolecular time and energy scales are sufficiently well separated that correlation functions involving both types of variables can be de-

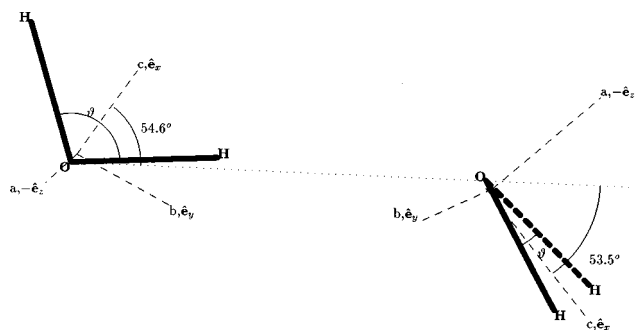


FIG. 1. Equilibrium configuration of a water dimer.

coupled at appropriate points. Also, it has been convenient to consider the hydrogen to oxygen mass ratio $M_H/M_O \sim 0.06$ to be sufficiently small to be treated as an expansion parameter when deriving commutation rules. Other small parameters involving thermal averages of relative mean square displacements are found numerically to be in the range of 0.01 to 0.1; these small parameters allow decoupling of various higher correlation functions. In Sec. II, we discuss two types of overtones, namely geometrical and mechanical overtones. Mechanical overtones are the direct result of the anharmonicity of confining Morse-oscillator potentials describing the covalent bond; geometrical overtones are due to the nonlinear relation between the electric dipole moment of the dimer and the local coordinates of the Morse potentials. Mixing of fundamentals and overtones is also discussed. There are two types of mixings, namely parallel-event and geometrical mixings. Parallel-event mixings are due to the fact that rotation of the dimer and intramolecular and intermolecular excitations happen simultaneously. Geometrical mixings result from the nonlinear relation between the electric dipole moment of the dimer and the local coordinates. These mixings between excitations transform absorption lines to bands and the mechanical overtones boost those low absorption bands to higher frequencies through parallel-event mixing. Results and conclusions follow in Secs. III and IV.

II. FORMALISM

A. Modeling of water dimer

The water dimer equilibrium structure is shown in Fig. 1. Of the 18 degrees of freedom, only those of the translational motion are trivial. The remaining 15 coupled degrees of freedom are very nontrivial, constituting a difficult “few-body” problem with important dynamics on several time scales. To a first approximation, these can be classified as six intramolecular vibrational modes, six strongly mixed intermolecular rotation-vibrational modes, and three degrees of freedom corresponding to overall rotation of the dimer. The six intermolecular rotation-vibrational modes can be regarded as basically manifestations of hindered rotations of the donor and acceptor H_2O groups, relative to each other. These intermolecular modes are expected to be strongly mixed, very anharmonic. We assume that the water molecule is sufficiently modeled¹⁹ by particles with local coordinates $s_{j\mu}$, three for each H_2O group, with effective mass matrix

m_{ij} moving in different Morse-oscillator potentials. The Hamiltonian operator, without the translational motion of the dimer, takes the form

$$H = \sum_{\mu=1}^2 \left[\sum_{i,j=1}^3 \frac{m_{ij} \dot{s}_{i\mu} \dot{s}_{j\mu}}{2} + H_r(\theta_{\mu}, \phi_{\mu}, \psi_{\mu}) \right] + H_R^D(\theta_D, \phi_D, \psi_D) + \sum_{\mu=1}^2 \left[\sum_{j=1}^3 D_j (1 - e^{-\alpha_j s_{j\mu}})^2 + f_{12} s_{1\mu} s_{2\mu} \right] + \frac{1}{2} \sum_{\mu \neq \nu} \sum_{j,k}^3 \Phi(\mathbf{x}_{j\mu}, \mathbf{x}_{k\nu}), \quad (1)$$

with

$$s_{(1,2)\mu} = R_{(1,2)\mu} \cos\left(\frac{\vartheta_{\mu} - \vartheta_0}{2}\right) - R_0, \quad (2)$$

$$s_{3\mu} = (R_{1\mu} + R_{2\mu}) \sin\left(\frac{\vartheta_{\mu} - \vartheta_0}{2}\right), \quad (3)$$

$R_{1\mu}$, $R_{2\mu}$ the two O–H bond lengths, ϑ_{μ} the included angle, H_R^D and H_r the rotational Hamiltonians of the water dimer and the μ th monomer, respectively, as a function of their own corresponding Eulerian angles $\theta_j^D = (\theta_D, \phi_D, \psi_D)$ and $\theta_{j\mu} = (\theta_{\mu}, \phi_{\mu}, \psi_{\mu})$ of their body axes ($\hat{\mathbf{e}}_x^{\mu}$, $\hat{\mathbf{e}}_y^{\mu}$, $\hat{\mathbf{e}}_z^{\mu}$) described in Fig. 1. The equilibrium Eulerian angles $\theta_{j\mu}^0$ are therefore¹⁶ $\theta_{j1}^0 = (0,0,0)$, $\theta_{j2}^0 = (3\pi/2, 0, 0.6\pi)$. $\mathbf{x}_{j\mu}$ are the Cartesian coordinates of the j th atoms, including the empirical negative point charge, of the μ th water molecules which is, of course, a function of the internal state variables $\theta_{j\mu}$'s and $s_{j\mu}$'s. The monomer indices are denoted by the Greek letters μ with $\mu=1$ for the acceptor molecule and $\mu=2$ for the donor molecule. The equilibrium bond length R_0 and angle ϑ_0 , empirical constants D_i and α_i , and the intermolecular interaction Φ are taken from the semiempirical model^{15,17} of Reimers *et al.* and they are $R_0 = 0.9572 \text{ \AA}$, $D_1 = D_2 = 131.250 \text{ kcal/mol}$, $D_3 = 98.27 \text{ kcal/mol}$, $\alpha_1 = \alpha_2 = 2.141 \text{ \AA}^{-1}$, $\alpha_3 = 0.706 \text{ \AA}^{-1}$, and $f_{12} = -15.1533 \text{ kcal mol}^{-1} \text{ \AA}^{-2}$. The first two terms on the right-hand side of Eq. (1) are the kinetic energy of each of the monomers observed at their centers of mass, with the first term describing the vibration restricted within the plane, which is defined by the location of those three atoms in the molecule, and the second term denoting the motion other than the in-plane vibration which we named loosely the off-plane motion. This off-plane motion is actually the rotational motion of the monomer about its center of mass. We use a rigid-body rotational kinematic term for both H_r and H_R^D because the in-plane vibration is very fast in comparison with the off-plane motion, as we will justify later in this section. This is due to the fact that the monomer is heavy and the dimer is loosely bounded, as opposed to the case in which the hydrogen is light and the covalent bond is strong. Thus

$$\begin{aligned}
 H_r(\theta_\mu, \phi_\mu, \psi_\mu) = & \frac{1}{2} \dot{\phi}_\mu^2 [I_a \sin^2 \psi_\mu + I_b \cos^2 \psi_\mu] \\
 & + \frac{1}{2} \dot{\theta}_\mu^2 [I_a \cos^2 \psi_\mu + I_b \sin^2 \psi_\mu] \\
 & + \frac{1}{2} I_c [\dot{\phi}_\mu \cos \theta_\mu + \dot{\psi}_\mu]^2 \\
 & + \dot{\phi}_\mu \dot{\theta}_\mu \sin \theta_\mu \sin \psi_\mu \cos \psi_\mu (I_a - I_b),
 \end{aligned} \tag{4}$$

where $I_a = 1.25 mR_0^2$, $I_b = 0.7 mR_0^2$, and $I_c = 2 mR_0^2$ are the moments of inertia about the principal axes of the monomer and m is the hydrogen mass. The rotational Hamiltonian for the dimer can also be obtained by having $\theta_\mu \rightarrow \theta_D$, $\phi_\mu \rightarrow \phi_D$, $\psi_\mu \rightarrow \psi_D$, $I_a \rightarrow I_a^D$, $I_b \rightarrow I_b^D$, $I_c \rightarrow I_c^D$, and $H_r \rightarrow H_r^D$ in the above equation. $I_a^D = 76.21 mR_0^2$, $I_b^D = 76.34 mR_0^2$ and $I_c^D = 2.51 mR_0^2$ are the principal moments of inertia of the dimer. The masses $m_j \equiv m_{jj}$ are obtained from the commutation relations $[\dot{s}_{j\mu}, s_{kv}(t_1)] = -i\hbar \delta_{\mu\nu} / m_{jk}$, which are derived from the commutation relations of those canonical variables of each atom in the molecule with

$$\begin{aligned}
 \frac{1}{m_1} = \frac{1}{m_2} = \frac{m+M}{mM}, \quad \frac{1}{m_{12}} = \frac{1}{m_{21}} = \frac{\cos \vartheta_0}{M}, \\
 \frac{1}{m_{13}} = -\frac{1}{m_{23}} = -\frac{\sin \vartheta_0}{M}, \quad \frac{1}{m_3} = 2 \left[\frac{1}{m_1} - \frac{\cos \vartheta_0}{M} \right],
 \end{aligned} \tag{5}$$

and M the oxygen mass. For simplicity, we assume $m \ll M$ and approximate $[\dot{s}_{j\mu}, s_{kv}] \approx -i\hbar \delta_{jk} \delta_{\mu\nu} / m_j$ with $m_1 = m_2 = m$ and $m_3 = m/2$. On the other hand, $\theta_{j\mu}$ are not conjugate to $\theta_{j\mu}$ and they are related to conjugate angular momentum operators L_θ^μ , L_ϕ^μ , and L_ψ^μ by

$$\begin{aligned}
 L_\theta^\mu = & (I_a \cos^2 \psi_\mu + I_b \sin^2 \psi_\mu) \dot{\theta}_\mu \\
 & + \sin \theta_\mu \sin \psi_\mu \cos \psi_\mu (I_a - I_b) \dot{\phi}_\mu,
 \end{aligned} \tag{6}$$

$$\begin{aligned}
 L_\phi^\mu = & (I_a \sin^2 \psi_\mu + I_b \cos^2 \psi_\mu) \dot{\phi}_\mu + \sin \psi_\mu \\
 & \times \cos \psi_\mu (I_a - I_b) \dot{\theta}_\mu + \cos \theta_\mu (\dot{\phi}_\mu + \dot{\psi}_\mu) I_c,
 \end{aligned} \tag{7}$$

$$L_\psi^\mu = I_c (\dot{\psi}_\mu + \dot{\phi}_\mu \cos \theta_\mu). \tag{8}$$

To simplify the situation, we consider the ratio

$$\delta = \frac{\langle \sin \theta_\mu \sin \psi_\mu \cos \psi_\mu \rangle (I_a - I_b)}{I_a \langle \cos^2 \psi_\mu \rangle + I_b \langle \sin^2 \psi_\mu \rangle} \tag{9}$$

for both the acceptor and donor molecules. The angle bracket represents the grand canonical average done at temperature T . For the acceptor molecule, this ratio is very small and for the donor molecule, it is of the order of 0.1 in the worst situation. Thus, we may assume $\delta \ll 1$ and obtain

$$[\dot{\theta}_{j\mu}, \theta_{kv}] \approx -i\hbar \delta_{\mu\nu} \left[\frac{\delta_{jk}}{I_{j\mu}} + \frac{\langle \cos \theta_\mu \rangle}{I_{2\mu}} (\delta_{j2} \delta_{k3} - \delta_{j3} \delta_{k2}) \right], \tag{10}$$

with

$$\begin{aligned}
 I_{1\mu} \approx & I_a \langle \cos^2 \psi_\mu \rangle + I_b \langle \sin^2 \psi_\mu \rangle \\
 = & I_a \cos^2 \psi_\mu^0 + I_b \sin^2 \psi_\mu^0,
 \end{aligned} \tag{11}$$

$$\begin{aligned}
 I_{2\mu} \approx & I_a \langle \sin^2 \psi_\mu \rangle + I_b \langle \cos^2 \psi_\mu \rangle \\
 = & I_a \sin^2 \psi_\mu^0 + I_b \cos^2 \psi_\mu^0,
 \end{aligned} \tag{12}$$

$$I_{3\mu} \approx \frac{I_c I_{2\mu}}{I_{2\mu} - I_c \langle \cos^2 \theta_\mu \rangle} = \frac{I_c I_{2\mu}}{I_{2\mu} - I_c \cos^2 \theta_\mu^0}. \tag{13}$$

Physically $s_{j\mu}$ describes the fast in-plane oscillation, with a period of order, \mathcal{T}_s , which has to negotiate with the strong O–H bond and the lone-electron pair from the oxygen atom. The resulting excitations are mainly intramolecular-like. On the other hand, the slow rotational motion of the monomers, described by $\theta_{j\mu}$ with a period \mathcal{T}_θ , is hindered by the weak interaction between monomers, thus it leads to intermolecular excitations. Due to the difference between the strength of a covalent bond and that of a hydrogen bond, $\mathcal{T}_s \ll \mathcal{T}_\theta$. Thus these off-plane rotations appear as static to the fast in-plane motion and have no significant effect; the off-plane rotations only see the time-average of those fast in-plane motions as if the atoms are stationary at their equilibrium positions within the plane. As a result, the rotation of the monomer can be sufficiently described by a rigid-body kinematic term in the Hamiltonian. However, the differentiation between intermolecular and rotational excitations of the dimer becomes difficult since I_c^D is of the same order as principal moments of inertia of the monomer. The rotation of the dimer along this axis can be as fast as the rotation of the monomer. The distance between centers of mass of two monomers can also vary. However, this variation is small. The movement of the oxygen atoms is easily counterbalanced by the low-energy motions of the hydrogen atoms. As a result, the distance between the centers of mass appears to be static within the time scale \mathcal{T}_θ . Thus there are two time scales associated with the rotation of the dimer, namely \mathcal{T}_c^D the period of rotation along the c axis, and \mathcal{T}_0^D the period of rotation along other axes. Judging from the magnitude of I_a^D and I_b^D , \mathcal{T}_0^D is much larger than \mathcal{T}_θ , therefore the rotation along these two axes can still be considered as rigid-body rotation, but not along the c axis. In other words, if we were to treat the dimer as a flexible cigar, the length should remain constant but the cigar is allowed to twist due to the internal rotation of the monomers. Strictly speaking, the dimer cannot be treated as an isolated rigid body within the time scale \mathcal{T}_θ . However, we can still use the rigid-body Hamiltonian for the kinematic term of the dimer with perturbation due to internal rotations. The effect of this internal motion amounts to severe broadening of rotational levels. Since we are interested in the broad band characteristic of the absorption spectrum, it is reasonable to adapt a semiclassical approach on the rotational excitations. We use a rigid-body Hamiltonian for the kinetic term to account for the rotation of the dimer as a whole and the transitions between different rotational states are evaluated quantum mechanically; however, the density of states of those rotational energy levels are taken to be continuous.

B. Absorption cross section of water dimer

The Hamiltonian in Eq. (1) is highly anharmonic in any of those state variables. Thus the incoming electromagnetic

radiation does not only excite fundamentals but also mechanical overtones which are geometry independent. These overtones only depend on the degree of anharmonicity of the potential in H and the amplitude of atomic vibrations, as we will discuss later in this paper. Besides this, mixing of fundamentals and overtones contributes to the absorption of solar radiation. This mixing is due to the fact that excitations, such as fundamentals and harmonics, rotational, intramolecular and intermolecular vibrations, all happen simultaneously. Further, there are in general other overtones and mixings, named here as geometrical overtones and mixings, which arise from those nonlinear terms in the state variables of the dipole interaction between the dimer and the electromagnetic field $\mathbf{E} = \mathbf{E}_0 \cos \omega t$, and they are geometry dependent. For instance, the dipole moment in the water molecule can align with \mathbf{E} by just changing the included angle and stretching R_1 and R_2 in the opposite directions. This is more effective, in other words faster in response, than rotating the molecule if the stretching amplitudes are large, and it is of course geometry dependent. These processes are included in the absorption cross section,

$$\sigma(\omega) = \frac{\omega}{6\pi\hbar} \sqrt{\frac{\mu_0}{\epsilon_0}} A_{\text{total}}(\omega), \quad (14)$$

where ω is the angular frequency of the randomly polarized electromagnetic field;

$$A_{\text{total}}(\omega) = \sum_{\mu, \bar{\mu}}^2 \sum_{a, \bar{a}}^3 \int_{-\infty}^{\infty} dt e^{i\omega t} \langle [p_{\mu}^a(t), p_{\bar{\mu}}^{\bar{a}}(0)] \rangle \quad (15)$$

is the spectral weight function of all excitations including overtones and mixing between excitations;

$$\mathbf{p}_{\alpha}(t) = \mathcal{R}(\theta_D(t), \phi_D(t), \psi_D(t)) \mathcal{R}(\theta_{\alpha}(t), \phi_{\alpha}(t), \psi_{\alpha}(t)) \times \mathbf{p}_{0\alpha}(t) \quad (16)$$

is the instantaneous dipole moment in the laboratory frame; \mathcal{R} is the rotational matrix, given in Appendix A, which describes the rotation of the instantaneous dipole moment of the monomer,

$$\mathbf{p}_{0\alpha}(t) = Q\gamma \left[(R_{1\alpha}(t) + R_{2\alpha}(t)) \cos\left(\frac{\vartheta_{\alpha}(t)}{2}\right) \hat{\mathbf{e}}_x^{\alpha} - (R_{1\alpha}(t) - R_{2\alpha}(t)) \sin\left(\frac{\vartheta_{\alpha}(t)}{2}\right) \hat{\mathbf{e}}_y^{\alpha} \right] \quad (17)$$

in the body-axis frame $(\hat{\mathbf{e}}_x^{\alpha}, \hat{\mathbf{e}}_y^{\alpha}, \hat{\mathbf{e}}_z^{\alpha})$, defined in Fig. 1, in terms of Eulerian angles of both the monomers and the dimer; $\gamma = 1 - d/R_0 \cos(\vartheta_0/2)$ with Q and d the same empirical constants obtained from Coker *et al.*¹⁴ The superscript of p_{μ}^i in Eq. (15) denotes the Cartesian components of \mathbf{p}_{μ} . For simplicity, we denote the rotational matrices for the dimer and the μ th monomer by \mathcal{R}^D and \mathcal{R}^{μ} , respectively.

C. Parallel-event mixings

All excitations are excited simultaneously and will be referred to as parallel events (in time). The intramolecular and other excitations can be considered as parallel events without any interference from one another since they are on

a different time scale. Further, we can also approximate $\langle [p_{\mu}^a(t), p_{\bar{\mu}}^{\bar{a}}(0)] \rangle \approx \langle [p_{\mu}^a(t), p_{\bar{\mu}}^{\bar{a}}(0)] \rangle \delta_{\mu\bar{\mu}}$ because the covalent bonds are very strong in comparison to the hydrogen bond. Thus the dipole moments of the acceptor and donor molecules are weakly correlated. On the other hand, intermolecular excitations do interfere with the rotational excitations of the dimer. However, within the regime of rigid-body approximation for the rotation of the dimer discussed in the last section, we can approximate them as noninterfering parallel events. Thus using this approximation in $A_{\text{total}}(\omega)$, rotational excitations and intermolecular and intramolecular excitations are all mixed, and their corresponding correlation functions appear as products in time t in the absorption cross section,

$$\begin{aligned} \sigma(\omega) \approx & \frac{Q^2 \gamma^2}{6\pi\hbar} \sqrt{\frac{\mu_0}{\epsilon_0}} \omega \sum \int_{-\infty}^{\infty} dt e^{i\omega t} \langle \mathcal{R}_{ab}^D(t) \mathcal{R}_{ab}^D(0) \rangle \\ & \times \langle \mathcal{R}_{bc}^{\mu}(t) \mathcal{R}_{bc}^{\mu}(0) \rangle \langle p_{0\mu}^c(t) p_{0\mu}^c(0) \rangle \\ & - \langle \mathcal{R}_{ab}^D(0) \mathcal{R}_{ab}^D(t) \rangle \langle \mathcal{R}_{bc}^{\mu}(0) \mathcal{R}_{bc}^{\mu}(t) \rangle \\ & \times \langle p_{0\mu}^c(0) p_{0\mu}^c(t) \rangle, \end{aligned} \quad (18)$$

where the summation sign is for all repeated indices. These parallel-event mixings among excitations are independent of the geometry of the water dimer because the instantaneous dipole moment can always be expressed in the form of Eq. (16).

We have used the fact that $\sum_a \langle \mathcal{R}_{ab}^D(t) \mathcal{R}_{ab}^D(0) \rangle = \sum_a \langle \mathcal{R}_{ab}^D(t) \mathcal{R}_{ab}^D(0) \rangle \delta_{bb}$ in obtaining Eq. (18) due to Eqs. (A24), (A25), and (A26), and the fact that \mathcal{R}^D is unitary. Each of these matrix elements is responsible for rotation of the dimer about a certain axis. For instance, the matrix elements $\langle \mathcal{R}_{ab}(t) \mathcal{R}_{ab}(0) \rangle$ for $a \neq 3 \neq b$ are responsible for the rotations about the a and the c axes which correspond to the $\Delta J = \pm 1$, $\Delta K = \pm 1$ transitions described in Refs. 29 and 30. As for $b=3$ and $a \neq 3$, the matrix elements are responsible for the rotations about the a axis, i.e., the $\Delta J = \pm 1$, $\Delta K = 0$ transitions. Both of these excitations occupy a narrow low-frequency range, named here as the NL branch, in the absorption spectrum due to the fact that the moment of inertia about the a axis is very large and therefore rotations about this axis are slow. On the other hand, for $a \neq 3$ and $b=3$, these matrix elements describe the rotation of the dimer about the c axis, i.e., the $\Delta J = 0$, $\Delta K = \pm 1$ transitions. The rotation about this axis is fast and therefore occupies a wider low-frequency range, named here as the WL branch, in the absorption spectrum. Further, the total equilibrium dipole moment of the dimer is almost parallel to the c axis, so the absorption of the NL branch is stronger than the WL branch. Detailed calculation shows that these two branches have approximately the same integrated absorption over respective frequency ranges. Therefore, we may simplify the dimer rotation correlation functions by averaging over the two branches. Further, $p_{0\mu}^1$ describes only the symmetric stretching mode $s_{1\mu} + s_{2\mu}$ and the bending mode $s_{3\mu}$, and $p_{0\mu}^2$ mainly the mixed mode $(s_{1\mu} - s_{2\mu})s_{3\mu}$ and asymmetric stretching mode $s_{1\mu} - s_{2\mu}$; they are orthogonal to each other if there is no interaction between H_2O groups. When the interaction between H_2O groups is switched on, these distinct

modes interact indirectly and thus $\langle p_{0\mu}^c(t)p_{0\mu}^{\bar{c}}(0) \rangle$ is small for $c \neq \bar{c}$, in comparison to the case when $c = \bar{c}$, and will be neglected. The sum over the monomer correlation function's indices can then be carried out exactly. We obtain

$$\sigma(\omega) = \frac{Q^2 \gamma^2}{6 \pi \hbar} \sqrt{\frac{\mu_0}{\epsilon_0}} \omega \sum_{\mu=1}^2 \int_{-\infty}^{\infty} dt e^{-i\omega t} [\mathcal{H}_{\mu}^{\gt}(t) \times \mathcal{F}_{\mu}^{\gt}(t) \mathcal{F}_{\text{av}}^{\gt}(t) - \mathcal{H}_{\mu}^{\lt}(t) \mathcal{F}_{\mu}^{\lt}(t) \mathcal{F}_{\text{av}}^{\lt}(t)] \quad (19)$$

with

$$\mathcal{H}_{\mu}^{\gt}(t) = R_0^2 \cos^2\left(\frac{\vartheta_0}{2}\right) + \int_{-\infty}^{\infty} \frac{d\omega}{2\pi} e^{-i\omega t} \chi_{\mu}(\omega) \left[\frac{1}{2} \pm \frac{1}{2} + n(\omega) \right] + G_{\mu}^{\gt}(t), \quad (20)$$

$$\mathcal{F}_{\mu}^{\gt}(t) = \frac{1}{2} \sum_c \sum_b^3 \langle (\mathcal{R}_{bc}^{\mu}(0) \mathcal{R}_{bc}^{\mu}(t))^{\gt} \rangle, \quad (21)$$

$$\mathcal{F}_{\text{av}}^{\gt}(t) = \frac{1}{2} \sum_{a,b}^3 (1 + \delta_{a3} \delta_{b3}) \langle (R_{ab}^D(t) R_{ab}^D(0))^{\gt} \rangle = \int_{-\infty}^{\infty} \frac{d\omega}{2\pi} e^{-i\omega t} \mathcal{F}_{\text{av}}(\omega) \left[\frac{1}{2} \pm \frac{1}{2} + n(\omega) \right], \quad (22)$$

where $\langle (\mathcal{R}_{ab}^D(t) \mathcal{R}_{ab}^D(0))^{\gt} \rangle = \mathcal{R}_{ab}^D(t) \mathcal{R}_{ab}^D(0)$ and $\langle (\mathcal{R}_{ab}^D(t) \mathcal{R}_{ab}^D(0))^{\lt} \rangle = \mathcal{R}_{ab}^D(0) \mathcal{R}_{ab}^D(t)$;

$$\chi_{\mu}(\omega) = A_{33}^{\mu\mu}(\omega) \sin^2\left(\frac{\vartheta_0}{2}\right) + \sum_{j,k}^2 A_{jk}^{\mu\mu}(\omega) \times [\delta_{jk} + (1 - \delta_{jk}) \cos \vartheta_0]$$

is the spectral weight function of all intramolecular excitations written in terms of spectral weight functions of the stretching and bending modes,

$$A_{jk}^{\mu\nu}(\omega) = \int_{-\infty}^{\infty} dt e^{i\omega t} \langle [s_{j\mu}(t), s_{k\nu}(0)] \rangle; \quad (23)$$

$\mathcal{F}_{\text{av}}(\omega)$ is the spectral weight function of overall rotational excitations of the dimer described in Appendix B and $n(\omega)$ is the Bose–Einstein distribution function. G_{μ}^{\gt} is given in the next section.

D. Geometrical overtones and mixings

The correlation functions $\langle \mathbf{p}_{0\mu}(t) \cdot \mathbf{p}_{0\mu}(0) \rangle$ contain correlation functions with order in $s_{j\mu}$ higher than the correlation function $\langle s_{j\mu}(t) s_{k\mu}(0) \rangle$ which is quadratic in $s_{j\mu}$. These extra anharmonic terms introduce geometrical mixings between intramolecular excitations and they are contained in the function

$$G_{\mu}^{\gt}(t) = \langle (s_{3\mu}(0) s_{3\mu}(t))^{\gt} \rangle N_{\mu-}^{\gt}(t) \sum_{j=0}^{\infty} C_j(n_+) \times \left[\frac{N_{\mu+}^{\gt}(t)}{4R_0^2} \right]^j, \quad (24)$$

where

$$N_{\mu\pm}^{\gt}(t) = \sum_{j=1}^2 \langle (s_{j\mu}(0) s_{j\mu}(t))^{\gt} \rangle \pm \sum_{j,k}^2 \langle (s_{j\mu}(0) s_{k\mu}(t))^{\gt} \rangle \times (1 - \delta_{jk}). \quad (25)$$

This series is obtained from decoupling $\Sigma_{j,\mu} \langle [p_{\mu}^j(t), p_{\mu}^j(0)] \rangle$ into an infinite series of intramolecular pair correlation functions. The leading C_j coefficients are given in Appendix A. Equation (24) shows that intramolecular excitations are mixed in a way similar to the parallel-event mixings. However, it is due to the nonlinearity in $s_{j\mu}$ of $\mathbf{p}_{0\mu}$, and the coefficients C_j are geometry dependent.

Similarly, anharmonic terms in rotational matrices also introduce geometrical overtones and mixings among intramolecular excitations. Expanding Eq. (21), we obtain

$$\mathcal{F}_{\mu}^{\gt}(t) = [1 + \cos^2 \theta_{1\mu}^0 F_{+}^{\gt}(\theta_{\mu}, t) + \sin^2 \theta_{1\mu}^0 F_{-}^{\gt}(\theta_{\mu}, t)] F^{\gt}(\psi_{\mu}, t) F^{\gt}(\phi_{\mu}, t), \quad (26)$$

with

$$F_{+}^{\gt}(x, t) = \sum_{j=0}^{\infty} B_{2j}(\langle x^2 \rangle) [\langle (x(0)x(t))^{\gt} \rangle]^{2j}, \quad (27)$$

$$F_{-}^{\gt}(x, t) = \sum_{j=0}^{\infty} B_{2j+1}(\langle x^2 \rangle) [\langle (x(0)x(t))^{\gt} \rangle]^{2j+1}, \quad (28)$$

$F^{\gt}(x, t) = F_{+}^{\gt}(x, t) + F_{-}^{\gt}(x, t)$ and B_j given in Appendix A. All these correlation functions require the knowledge of correlation functions $\langle s_{j\mu}(t_1) s_{k\nu}(t_2) \rangle$, $\langle s_{k\nu}(t_2) s_{j\mu}(t_1) \rangle$, $\langle \theta_{j\mu}(t_1) \theta_{k\nu}(t_2) \rangle$, $\langle \theta_{k\nu}(t_2) \theta_{j\mu}(t_1) \rangle$, $\langle R_{ij}^D(t_1) R_{ij}^D(t_2) \rangle$, and $\langle R_{ij}^D(t_2) R_{ij}^D(t_1) \rangle$ which are obtained from the solutions of their nonlinear equations of motion.

E. Nonlinear equations of motion and mechanical overtones

With the commutation relations from Eqs. (5) and (10), we have coupled equations of motion for these correlation functions in the imaginary time domain,³¹

$$m_j \frac{\partial^2}{\partial t_1^2} \langle (s_{j\mu}(t_1) s_{k\nu}(t_2))_+ \rangle + 2\alpha_j D_j \langle (e^{-\alpha_j s_{k\nu}(t_1)} \times (1 - e^{-\alpha_j s_{j\mu}(t_1)}) s_{k\nu}(t_2))_+ \rangle + i \int_0^{-i\beta} dt_3 \times \sum_{n,\epsilon} [U_{jn}^{\mu\epsilon}(t_1 - t_3) \langle (s_{n\epsilon}(t_3) s_{k\nu}(t_2))_+ \rangle + \bar{V}_{jn}^{\mu\epsilon}(t_1 - t_3) \langle (\theta_{n\epsilon}(t_3) s_{k\nu}(t_2))_+ \rangle] = -i\hbar \delta_{jk} \delta_{\mu\nu} \delta(t_1 - t_2) - f_{12} (\delta_{j1} \delta_{k'2} + \delta_{j2} \delta_{k'1}) \times \langle (s_{k\mu}(t_1) s_{k'\nu}(t_2))_+ \rangle, \quad (29)$$

$$\begin{aligned}
I_{j\mu} \frac{\partial^2}{\partial t_1^2} \langle (\theta_{j\mu}(t_1) \theta_{k\nu}(t_2))_+ \rangle + i \int_0^{-i\beta} dt_3 \sum_{n,\epsilon} [V_{jn}^{\mu\epsilon}(t_1 - t_3) \\
\times \langle (\theta_{n\epsilon}(t_3) \theta_{k\nu}(t_2))_+ \rangle + \bar{U}_{jn}^{\mu\epsilon}(t_1 - t_3) \\
\times \langle (s_{n\epsilon}(t_3) \theta_{k\nu}(t_2))_+ \rangle] \\
= -i\hbar \delta_{jk} \delta_{\mu\nu} \delta(t_1 - t_2), \quad (30)
\end{aligned}$$

where

$$U_{jn}^{\alpha\beta}(t_1 - t_3) = \sum_{l,m} \sum_{\mu} \int d\mathbf{r} \mathbf{J}_{j\alpha}^m \cdot \nabla \Phi_{ml}^{\alpha\mu}(\mathbf{r}) \frac{\delta g_{ml}^{\alpha\mu}(\mathbf{r}, t_1)}{\delta \langle s_{n\beta}(t_3) \rangle}, \quad (31)$$

$$\bar{U}_{jn}^{\alpha\beta}(t_1 - t_3) = \sum_{l,m} \sum_{\mu} \int d\mathbf{r} \mathbf{L}_{j\alpha}^m \cdot \nabla \Phi_{ml}^{\alpha\mu}(\mathbf{r}) \frac{\delta g_{ml}^{\alpha\mu}(\mathbf{r}, t_1)}{\delta \langle s_{n\beta}(t_3) \rangle}, \quad (32)$$

$$V_{jn}^{\alpha\beta}(t_1 - t_3) = \sum_{l,m} \sum_{\mu} \int d\mathbf{r} \mathbf{L}_{j\alpha}^m \cdot \nabla \Phi_{ml}^{\alpha\mu}(\mathbf{r}) \frac{\delta g_{ml}^{\alpha\mu}(\mathbf{r}, t_1)}{\delta \langle \theta_{n\beta}(t_3) \rangle}, \quad (33)$$

$$\bar{V}_{jn}^{\alpha\beta}(t_1 - t_3) = \sum_{l,m} \sum_{\mu} \int d\mathbf{r} \mathbf{J}_{j\alpha}^m \cdot \nabla \Phi_{ml}^{\alpha\mu}(\mathbf{r}) \frac{\delta g_{ml}^{\alpha\mu}(\mathbf{r}, t_1)}{\delta \langle \theta_{n\beta}(t_3) \rangle}, \quad (34)$$

with

$$\mathbf{J}_{j\alpha}^m = \vec{\mathcal{R}}(\theta_\alpha^0, \phi_\alpha^0, \psi_\alpha^0) \left\langle \frac{\partial \mathbf{r}_{m\alpha}}{\partial s_{j\alpha}} \right\rangle, \quad (35)$$

$$\begin{aligned}
\mathbf{L}_{j\alpha}^m = \sum_k \left\langle \frac{\partial \vec{\mathcal{R}}(\theta_\alpha, \phi_\alpha, \psi_\alpha)}{\partial \theta_{j\alpha}} \right\rangle \langle \mathbf{r}_{m\alpha} \rangle \\
\times \left[\delta_{jk} + \cos \theta_{1\alpha}^0 \frac{I_{j\alpha}}{I_{2\alpha}} (\delta_{j2} \delta_{k3} - \delta_{j3} \delta_{k2}) \right], \quad (36)
\end{aligned}$$

$$g_{ml}^{\alpha\mu}(\mathbf{r}, t) = \langle \delta(\mathbf{r} - \mathbf{r}_{m\alpha}(t) + \mathbf{r}_{l\mu}(t)) \rangle, \quad (37)$$

the pair distribution function between the m th atom of the α th molecule and the l th atom, including the negative point charge, of the μ th molecule, and $\beta = (k_B T)^{-1}$ the inverse temperature. The time-ordered operation of $s_{j\mu}(t)$ and $s_{k\nu}(0)$ in the imaginary time domain is defined as $(s_{j\mu}(t) s_{k\nu}(0))_+ = s_{j\mu}(t) s_{k\nu}(0)$ for $-\beta < \text{Im}(t) < 0$ and $(s_{j\mu}(t) s_{k\nu}(0))_+ = s_{k\nu}(0) s_{j\mu}(t)$ for $0 < \text{Im}(t) < \beta$. The index m runs from 1 to 4 with 1 and 2 for those two hydrogen atoms, 3 for the oxygen atom and 4 for the negative point charge described by Coker *et al.* The vector $\mathbf{r}_{m\alpha}$, given in Appendix A, is the position vector of the m th atom of the α molecule with respect to the body-axis frame about their individual centers of mass. The communication between the slow intermolecular and fast intramolecular excitations are mainly through the correlation function $\langle s_{j\mu}(t) \theta_{k\nu}(0) \rangle$ which is ignored in our calculation due to the fact that $\langle s_{j\mu}(t) \theta_{k\nu}(0) \rangle \approx \langle s_{j\mu}(t) \rangle \langle \theta_{k\nu}(0) \rangle = 0$. In fact, we estimate that $R_0(\omega_{\text{intra}}^2 - \omega_{\text{inter}}^2) \langle s \theta \rangle \sim \omega_{\text{inter}}^2 \langle s s \rangle$ by inspecting the equation of motion of $\langle s_{j\mu}(t) \theta_{k\nu}(0) \rangle$ where ω_{inter} and ω_{intra} are, respectively, the frequencies of the intermolecular and intramolecular excitations.

Here we follow Horner's treatment³²⁻³⁵ of solid helium and assume that the pair distribution functions¹⁹ are function-

als of both $\langle s_{j\mu}(t) \rangle$ and $\langle \theta_{j\mu}(t) \rangle$ explicitly and implicitly through $\langle (s_{j\mu}(t) s_{k\nu}(t))_+ \rangle$ and $\langle (\theta_{j\mu}(t) \theta_{k\nu}(t)) \rangle$. Thus

$$\begin{aligned}
\frac{\delta g_{mk}^{\alpha\mu}(\mathbf{r}_1, t_1)}{\delta \langle s_{n\nu}(t_3) \rangle} \approx \frac{\delta g_{mk}^{\alpha\mu}(\mathbf{r}_1, t_1)}{\delta \langle s_{n\nu}(t_1) \rangle} \delta(t_1 - t_3) \\
+ \sum_{i,j} \sum_{\gamma,\epsilon} \frac{\delta g_{mk}^{\alpha\mu}(\mathbf{r}_1, t_1)}{\delta \langle (s_{i\gamma}(t_1) s_{j\epsilon}(t_1))_+ \rangle} \\
\times \langle (s_{i\gamma}(t_1) s_{n\nu}(t_3))_+ \rangle \\
\times \langle (s_{n\nu}(t_3) s_{j\epsilon}(t_1))_+ \rangle, \quad (38)
\end{aligned}$$

$$\begin{aligned}
\frac{\delta g_{mk}^{\alpha\mu}(\mathbf{r}_1, t_1)}{\delta \langle \theta_{n\nu}(t_3) \rangle} \approx \frac{\delta g_{mk}^{\alpha\mu}(\mathbf{r}_1, t_1)}{\delta \langle \theta_{n\nu}(t_1) \rangle} \delta(t_1 - t_3) \\
+ \sum_{i,j} \sum_{\gamma,\epsilon} \frac{\delta g_{mk}^{\alpha\mu}(\mathbf{r}_1, t_1)}{\delta \langle (\theta_{i\gamma}(t_1) \theta_{j\epsilon}(t_1))_+ \rangle} \\
\times \langle (\theta_{i\gamma}(t_1) \theta_{n\nu}(t_3))_+ \rangle \\
\times \langle (\theta_{n\nu}(t_3) \theta_{j\epsilon}(t_1))_+ \rangle, \quad (39)
\end{aligned}$$

with

$$\begin{aligned}
\sum_{l,m} \sum_{\mu} \int d\mathbf{r} \mathbf{J}_{j\alpha}^m \cdot \nabla \Phi_{ml}^{\alpha\mu}(\mathbf{r}) \frac{\delta g_{ml}^{\alpha\mu}(\mathbf{r}, t_1)}{\delta \langle s_{n\beta}(t_1) \rangle} \\
= \sum_{l,m} \sum_{\mu} \int d\mathbf{r} g_{ml}^{\alpha\mu}(\mathbf{r}, t_1) (\mathbf{J}_{n\alpha}^m \delta_{\alpha\beta} - \mathbf{J}_{n\mu}^l \delta_{\mu\beta}) \\
\cdot \nabla [\mathbf{J}_{j\alpha}^m \cdot \nabla \Phi_{ml}^{\alpha\mu}(\mathbf{r})] \equiv -b_{jn}^{\alpha\beta}, \quad (40)
\end{aligned}$$

$$\begin{aligned}
\sum_{l,m} \sum_{\mu} \int d\mathbf{r} \mathbf{L}_{j\alpha}^m \cdot \nabla \Phi_{ml}^{\alpha\mu}(\mathbf{r}) \frac{\delta g_{ml}^{\alpha\mu}(\mathbf{r}, t_1)}{\delta \langle \theta_{n\beta}(t_1) \rangle} \\
= \sum_{l,m} \sum_{\mu} \int d\mathbf{r} g_{ml}^{\alpha\mu}(\mathbf{r}, t_1) (\mathbf{L}_{n\alpha}^m \delta_{\alpha\beta} - \mathbf{L}_{n\mu}^l \delta_{\mu\beta}) \\
\cdot \nabla [\mathbf{L}_{j\alpha}^m \cdot \nabla \Phi_{ml}^{\alpha\mu}(\mathbf{r})] \equiv -e_{jn}^{\alpha\beta}, \quad (41)
\end{aligned}$$

$$\begin{aligned}
\sum_{l,m} \sum_{\mu} \int d\mathbf{r} \mathbf{J}_{j\alpha}^m \cdot \nabla \Phi_{ml}^{\alpha\mu}(\mathbf{r}) \frac{\delta g_{ml}^{\alpha\mu}(\mathbf{r}, t_1)}{\delta \langle (s_{i\gamma}(t_1) s_{k\epsilon}(t_1))_+ \rangle} \\
= \frac{1}{4} \sum_{l,m} \sum_{\mu} \int d\mathbf{r} g_{ml}^{\alpha\mu}(\mathbf{r}, t_1) (\mathbf{J}_{i\alpha}^m \delta_{\alpha\gamma} - \mathbf{J}_{i\mu}^l \delta_{\mu\gamma}) \\
\cdot \nabla (\mathbf{J}_{k\alpha}^m \delta_{\alpha\epsilon} - \mathbf{J}_{k\mu}^l \delta_{\mu\epsilon}) \cdot \nabla [\mathbf{J}_{j\alpha}^m \cdot \nabla \Phi_{ml}^{\alpha\mu}(\mathbf{r})] \\
\equiv -\frac{1}{4} d_{jki}^{\alpha\epsilon\gamma}, \quad (42)
\end{aligned}$$

$$\begin{aligned}
\sum_{l,m} \sum_{\mu} \int d\mathbf{r} \mathbf{L}_{j\alpha}^m \cdot \nabla \Phi_{ml}^{\alpha\mu}(\mathbf{r}) \frac{\delta g_{ml}^{\alpha\mu}(\mathbf{r}, t_1)}{\delta \langle (\theta_{i\gamma}(t_1) \theta_{k\epsilon}(t_1))_+ \rangle} \\
= \frac{1}{4} \sum_{l,m} \sum_{\mu} \int d\mathbf{r} g_{ml}^{\alpha\mu}(\mathbf{r}, t_1) (\mathbf{L}_{i\alpha}^m \delta_{\alpha\gamma} - \mathbf{L}_{i\mu}^l \delta_{\mu\gamma}) \\
\cdot \nabla (\mathbf{L}_{k\alpha}^m \delta_{\alpha\epsilon} - \mathbf{L}_{k\mu}^l \delta_{\mu\epsilon}) \cdot \nabla [\mathbf{L}_{j\alpha}^m \cdot \nabla \Phi_{ml}^{\alpha\mu}(\mathbf{r})] \\
\equiv -\frac{1}{4} f_{jki}^{\alpha\epsilon\gamma}. \quad (43)
\end{aligned}$$

With the above equations, Eqs. (29) and (30) are closed as long as we have information on the pair distribution functions. We use a cone-of-sight approximation such that

$$g_{ml}^{\alpha\mu}(\mathbf{r},t) \approx \bar{g}_{ml}^{\alpha\mu}(r) \quad \text{for } \varphi_{ml}^{\alpha\mu}(\mathbf{r}) < \frac{\Delta_{ml}^{\alpha\mu}}{2r},$$

$$\approx 0 \quad \text{otherwise,} \tag{44}$$

with $\bar{g}_{ml}^{\alpha\mu}(r)$ the normalized pair distribution functions obtained from Coker *et al.*,¹⁹ $\Delta_{ml}^{\alpha\mu}$ the half-width of $\bar{g}_{ml}^{\alpha\mu}(r)$, and $\varphi_{ml}^{\alpha\mu}(\mathbf{r})$ the angle between \mathbf{r} and the equilibrium $\mathbf{r}_{m\alpha}^0 - \mathbf{r}_{l\mu}^0$. The introduction of complex time t_3 above is just one of the convenient ways to deal with the entanglement between the time-evolution operator e^{-iHt} and the statistical weight $e^{-\beta H}$ in the grand canonical average. The equations of motion, Eqs. (29) and (30), have such a form that each state variable has either an assigned mass m_j or moment of inertia $I_{j\mu}$, so $U_{jn}^{\alpha\beta}$ and $\bar{V}_{jn}^{\alpha\beta}$ can be interpreted as generalized dynamical matrices describing forces acting on the $s_{j\mu}$ mode with m_j by other intramolecular and intermolecular excitations, respectively; similarly, $V_{jn}^{\alpha\beta}$ and $\bar{U}_{jn}^{\alpha\beta}$ describe the torque acting on the $\theta_{j\mu}$ mode with moment of inertia $I_{j\mu}$ due to other intermolecular and intramolecular excitations.

The equation of motion for the intramolecular excitation is very similar to that of the intermolecular excitation, except that there is an extra term on the left-hand side of Eq. (29) due to the restoring force of the confining Morse-oscillator potential. It is this term, together with the U and \bar{V} terms, which gives the fundamental of those intramolecular excitations if only the second order term in $s_{j\mu}$ of the Morse-oscillator potential is kept; because of its anharmonicity, in other words, higher order term in $s_{j\mu}$, it also leads to overtones of these fundamentals. To see this, we expand the second term on the left-hand side of Eq. (29) in terms of correlation functions of different orders in $s_{j\mu}(t_1)$,

$$\begin{aligned} & \langle (e^{-\alpha_j s_{j\mu}(t_1)} (1 - e^{-\alpha_j s_{j\mu}(t_1)}) s_{j\mu}(t_2))_+ \rangle \\ & - \alpha_j \langle (s_{j\mu}(t_1) s_{j\mu}(t_2))_+ \rangle \\ & = -\alpha_j \left[\frac{3}{2} \alpha_j \langle (s_{j\mu}(t_1) s_{j\mu}(t_1) s_{j\mu}(t_2))_+ \rangle \right. \\ & \quad - \frac{7}{6} \alpha_j^2 \langle (s_{j\mu}(t_1) s_{j\mu}(t_1) s_{j\mu}(t_1) s_{j\mu}(t_2))_+ \rangle \\ & \quad \left. + \frac{5}{8} \alpha_j^3 \langle (s_{j\mu}(t_1) s_{j\mu}(t_1) s_{j\mu}(t_1) s_{j\mu}(t_1) s_{j\mu}(t_2))_+ \rangle + \dots \right]. \end{aligned} \tag{45}$$

However, we cannot truncate the series even for small $s_{j\mu}$ since the correlation functions involve two different time arguments. To do so will eliminate all overtones. To see this, we consider the easiest situation when $U_{jn}^{\alpha\beta} = \bar{V}_{jn}^{\alpha\beta} = 0$ and α_j is so small that the right-hand side of the above equation can be considered as zero. This is the case when we have the Morse-oscillator potential reduced to a simple harmonic-oscillator potential with a harmonic frequency $\omega_j = \sqrt{2\alpha_j^2 D_j / m_j}$. It becomes obvious when the second term on the left-hand side of Eq. (45) is substituted into Eq. (29). This harmonic motion is of course independent of $\langle s_{j\mu}(t) \rangle$ and it contains no higher harmonics. If we allow α_j to increase by a small amount, it is no longer linear, but this periodic motion can still be described, within a certain time π/ω_j , by a quasistatic harmonic potential as a function of the instantaneous $\langle s_{j\mu} \rangle$. On average it gives a different harmonic frequency which depends on $n_j^\mu \equiv \langle s_{j\mu}^2 \rangle$, but this static treatment does not contain any overtones. We refer to the

term obtained from this treatment as the local term in time. On the other hand, if α_j is increased further, the mechanical motion cannot sufficiently be described by the instantaneous $\langle s_{j\mu} \rangle$ alone but also the $\langle s_{j\mu} \rangle$ at a different time within π/ω_j . Proper consideration of this will lead to a term which we refer to as the nonlocal term in time. It is this nonlocal term which gives rise to all other overtones.

Again, we use Horner's method and express each correlation function in Eq. (45) in terms of the local and nonlocal parts and ignore all those higher order terms beyond $\alpha_j^4 n_j^{\mu 2}$, since $\alpha_1^2 n_1^\mu \sim 0.01$ and $\alpha_3^2 n_3^\mu \sim 0.001$ in our case. From this, we obtain

$$\begin{aligned} & \langle (s_{j\mu}(t_1) s_{j\mu}(t_1) s_{j\mu}(t_2))_+ \rangle - \frac{3}{2} \alpha_j n_j^\mu \left(1 - \frac{7}{6} \alpha_j^2 n_j^{\mu 2} \right) \\ & \times \langle (s_{j\mu}(t_1) s_{j\mu}(t_2))_+ \rangle \\ & \approx i \frac{3\alpha_j m_j \omega_j^2}{2\hbar} \int dt_3 \langle (s_{j\mu}(t_1) s_{j\mu}(t_3))_+ \rangle \\ & \times \langle (s_{j\mu}(t_1) s_{j\mu}(t_3))_+ \rangle \langle (s_{j\mu}(t_3) s_{j\mu}(t_2))_+ \rangle, \end{aligned} \tag{46}$$

$$\begin{aligned} & \langle (s_{j\mu}(t_1) s_{j\mu}(t_1) s_{j\mu}(t_1) s_{j\mu}(t_1) s_{j\mu}(t_2))_+ \rangle \\ & - \frac{3}{2} \alpha_j n_j^{\mu 2} \langle (s_{j\mu}(t_1) s_{j\mu}(t_2))_+ \rangle \\ & \approx i \frac{18n_j^\mu \alpha_j m_j \omega_j^2}{\hbar} \int dt_3 \langle (s_{j\mu}(t_1) s_{j\mu}(t_3))_+ \rangle \\ & \times \langle (s_{j\mu}(t_1) s_{j\mu}(t_3))_+ \rangle \langle (s_{j\mu}(t_3) s_{j\mu}(t_2))_+ \rangle, \end{aligned} \tag{47}$$

and

$$\begin{aligned} & \langle (s_{j\mu}(t_1) s_{j\mu}(t_1) s_{j\mu}(t_1) s_{j\mu}(t_2))_+ \rangle \\ & \approx n_j^\mu \langle (s_{j\mu}(t_1) s_{j\mu}(t_2))_+ \rangle. \end{aligned} \tag{48}$$

Thus Eqs. (29) and (30) are simplified to

$$\begin{aligned} & m_j \left\{ \frac{\partial^2}{\partial t_1^2} + \sum_{n,\epsilon} [(\omega_j^2 - v_{j\mu}) \delta_{jn} \delta_{\mu\epsilon} - b_{jn}^{\mu\epsilon}] \right\} \\ & \times \langle (s_{n\epsilon}(t_1) s_{k\nu}(t_2))_+ \rangle - \sum_{n,\epsilon} e_{jn}^{\mu\epsilon} \langle (\theta_{n\epsilon}(t_1) s_{k\nu}(t_2))_+ \rangle \\ & + f_{12} \delta_{\mu\nu} (\delta_{j1} \delta_{k2} - \delta_{j2} \delta_{k1}) \langle (s_{k\mu}(t_1) s_{j\mu}(t_2))_+ \rangle \\ & + im_j \int_0^{-i\beta} dt_3 M_{j\mu}(t_1 - t_3) \langle (s_{j\mu}(t_3) s_{j\mu}(t_2))_+ \rangle \\ & + i \int_0^{-i\beta} dt_3 \sum_{n,\epsilon} \mathcal{W}_{jn}^{\mu\epsilon}(t_1 - t_3) \langle (s_{n\epsilon}(t_3) s_{k\nu}(t_2))_+ \rangle \\ & = -i\hbar \delta_{jk} \delta_{\mu\nu} \delta(t_1 - t_2), \end{aligned} \tag{49}$$

$$\begin{aligned}
I_{j\mu} & \left(\frac{\partial^2}{\partial t_1^2} - \sum_{n,\epsilon} e_{jn}^{\mu\epsilon} \right) \langle (\theta_{n\epsilon}(t_1) \theta_{k\nu}(t_2))_+ \rangle \\
& - \sum_{n,\epsilon} b_{jn}^{\mu\epsilon} \langle (s_{n\epsilon}(t_1) \theta_{k\nu}(t_2))_+ \rangle \\
& + i \int_0^{-i\beta} dt_3 \sum_{n,\epsilon} \mathcal{Z}_{jn}^{\mu\epsilon}(t_1 - t_3) \langle (\theta_{n\epsilon}(t_3) \theta_{k\nu}(t_2))_+ \rangle \\
& = -i\hbar \delta_{jk} \delta_{\mu\nu} \delta(t_1 - t_2), \tag{50}
\end{aligned}$$

with

$$v_{j\mu} = \frac{13}{12} \omega_j^2 \alpha_j^2 n_{j\mu} - \frac{27}{16} \omega_j^2 \alpha_j^4 n_{j\mu}^2 \tag{51}$$

the local term, and nonlocal terms

$$\begin{aligned}
M_{j\mu}(t_1 - t_2) & = \left(\frac{3}{2} \alpha_j \omega_j^2 \right)^2 \frac{m_j}{\hbar} \langle (s_{j\mu}(t_1) s_{j\mu}(t_2))_+ \rangle \\
& \times \langle (s_{j\mu}(t_1) s_{j\mu}(t_2))_+ \rangle, \tag{52}
\end{aligned}$$

$$\begin{aligned}
\mathcal{L}_{jn}^{\mu\epsilon}(t_1 - t_2) & = \frac{1}{4} \sum d_{jil}^{\mu\nu\gamma} d_{pqn}^{\eta\phi\epsilon} \langle (s_{l\gamma}(t_1) s_{p\eta}(t_3))_+ \rangle \\
& \times \langle (s_{q\phi}(t_1) s_{i\nu}(t_3))_+ \rangle, \tag{53}
\end{aligned}$$

$$\begin{aligned}
\mathcal{Z}_{jn}^{\mu\epsilon}(t_1 - t_2) & = \frac{1}{4} \sum f_{jil}^{\mu\nu\gamma} f_{pqn}^{\eta\phi\epsilon} \langle (\theta_{l\gamma}(t_1) \theta_{p\eta}(t_3))_+ \rangle \\
& \times \langle (\theta_{q\phi}(t_1) \theta_{i\nu}(t_3))_+ \rangle. \tag{54}
\end{aligned}$$

The term $(\omega_j^2 - v_{j\mu}) \delta_{jn} \delta_{\mu\epsilon} - b_{jn}^{\mu\epsilon}$ in Eq. (49) after matrix diagonalization can be interpreted as the location of those local mode frequencies with $v_{j\mu}$ the modification of harmonic frequency squared ω_j^2 due to the anharmonic nature of the Morse potential, and $b_{jn}^{\mu\epsilon}$ the frequency squared shift due to the interaction between the acceptor and the donor molecules. Nonlocal term \mathcal{L} introduces broadening in intramolecular excitations and $M_{j\mu}$ leads to intramolecular overtones. There is a distinction between broadening and overtones in these intramolecular excitations because the lifetime of these excitations is very long. On the other hand, the lifetime of intermolecular excitations is very short. Broadening and overtones are indistinguishable; both are manifested in \mathcal{Z} of Eq. (50). The location of intermolecular excitations is designated by $e_{jn}^{\mu\epsilon}$ after matrix diagonalization. The two sets of coupled Dyson equations, Eqs. (49) and (50), have been solved numerically and self-consistently. We obtain

$$\begin{aligned}
A_{jj}^{\mu\mu}(\omega) & = 2G_{jk}^{\mu\epsilon}(\omega + i0^+) G_{lj}^{\nu\mu}(\omega - i0^+) \text{Im} \left[\sum_{0kl}^{\epsilon\nu} (\omega + i0^+) \right. \\
& \left. + M_{j\mu}(\omega + i0^+) \delta_{jk} \delta_{kl} \delta_{\mu\epsilon} \delta_{\epsilon\nu} \right], \tag{55}
\end{aligned}$$

where $\Sigma_0 + M$ is the total self-energy matrix. $G_{jk}^{\mu\nu}(\omega \pm i0^+)$, $M_{j\mu}(\omega + i0^+)$, and $\Sigma_{kl0}^{\nu\epsilon}(\omega + i0^+)$ denote the analytic continuations of propagators and self-energy from Matsubara frequencies to the real ω axis. The spectral weight function $A_{jj0}^{\mu\mu}(\omega)$ obtained from Eq. (55) with $\text{Im}[M_{j\mu}(\omega + i0^+)] = 0$ is approximately equal to the spectral weight function of the fundamentals. With this approximation,

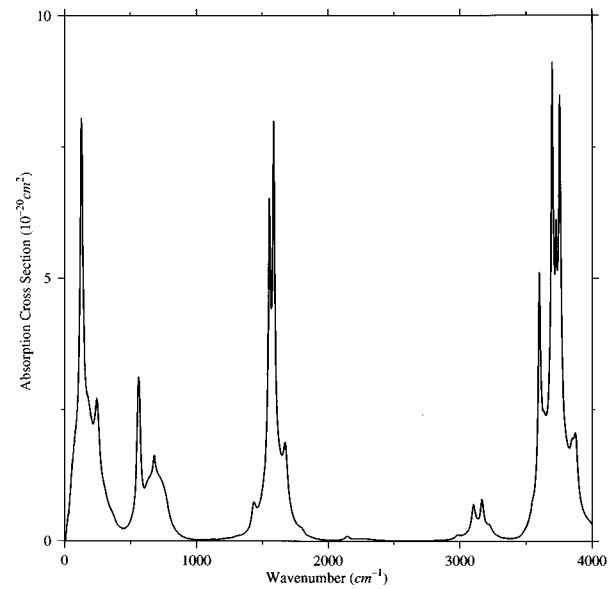


FIG. 2. Absorption cross section of water dimer due to fundamentals as a function of wave number.

which is valid as long as the lifetime of intramolecular excitations is very long in comparison to their inverse frequency, we have

$$G_{jj\pm}^{\mu\mu}(\omega) \approx \int_{-\infty}^{\infty} \frac{d\omega_1}{2\pi} \frac{A_{jj0}^{\mu\mu}(\omega - \omega_1)}{\omega_1 \pm i0^+} \equiv G_{jj0\pm}^{\mu\mu}(\omega), \tag{56}$$

and therefore

$$\begin{aligned}
A_{jj}^{\mu\mu}(\omega) & \approx A_{jj0}^{\mu\mu}(\omega) + G_{jj0+}^{\mu\mu}(\omega) G_{jj0-}^{\mu\mu}(\omega) \\
& \times \text{Im}[M_j^{\mu}(\omega + i0^+)], \tag{57}
\end{aligned}$$

where

$$\begin{aligned}
\text{Im}[M_j^{\mu}(\omega + i0^+)] & = \left(\frac{3}{2} \frac{\alpha_j \omega_j^2 m_j}{\hbar} \right)^2 \int_{-\infty}^{\infty} \frac{d\omega_1}{2\pi} \\
& \times A_{jj}^{\mu\mu}(\omega_1) A_{jj}^{\mu\mu}(\omega - \omega_1) [1 + n(\omega_1) \\
& + n(\omega - \omega_1)]. \tag{58}
\end{aligned}$$

Equations (57) and (58) yield an integral equation which can be self-consistently solved to obtain the full spectral weight function of the intramolecular fundamentals and its mechanical overtones.

III. RESULTS AND DISCUSSIONS

The equations of motion for both the intramolecular and intermolecular fundamentals are solved self-consistently and the corresponding absorption cross section is shown in Fig. 2. There are six intramolecular fundamentals, three from the acceptor molecule and three from the donor molecule; the smallest peak near 3000 cm^{-1} is the first harmonic and combination of the bending modes. They are all broadened by the dimer rotation, parallel-event, and geometrical mixings among all excitations including intermolecular overtones. In addition to these broadenings, the low-frequency intermolecular fundamentals are also broadened heavily due to the anharmonicity of the intermolecular interaction. In compari-

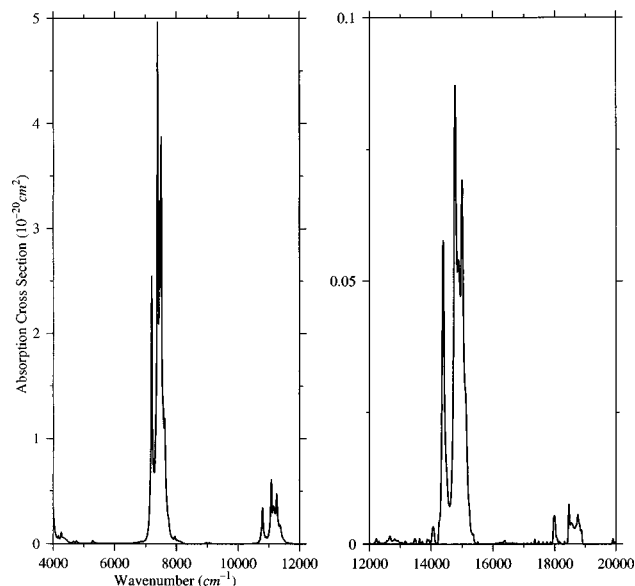


FIG. 3. Absorption cross section of water dimer due to overtones as a function of wave number.

son with the experimental values of those vibrational lines, the accuracy is about 4%. As for the intermolecular modes, the acceptor modes have comparable accuracy but the donor modes are consistently higher than experimental values.

Figure 3 shows mechanical overtones beyond 4000 cm^{-1} . They are both geometrical and parallel-event mixed with all other intermolecular and intramolecular excitations of both fundamentals and overtones. These overtones are quite strong because the time-averaged movement of the hydrogen atoms done within $\delta t < \omega_{\text{intra}}^{-1}$ is very large, or in other words, the broadening of the intramolecular excitations is large and the binding potentials are very anharmonic. Since intramolecular fundamentals have frequencies large in comparison to intermolecular fundamentals, these mechanical overtones anchor and boost the intermolecular modes to higher frequencies through parallel-event mixing. Therefore, the absorption spectrum forms a continuum around the mechanical overtones of those stretching and bending modes. The broadening effect is more pronounced for higher harmonics because there are more excitations to be mixed at high frequencies.

Combinations between different intramolecular modes are very weak but still observable in Fig. 4. The absorption cross section decreases exponentially with frequency for both the water dimer and water monomer. However, the dimer absorption cross section decreases more slowly than that of the monomer,^{36,37} as shown in Fig. 4. It is essential to note that there are shifts in frequency for the dimer relative to the water monomer. Both water monomers and dimers are present in the earth's atmosphere and they absorb solar radiation in different frequency ranges. This is especially important in the higher frequency range where the intensity of solar radiation is high. In this range, the absorption of solar radiation by water monomer is weak. This difference in the decay rate suggests that the water dimer may play a role in the radiation budget of the earth's atmosphere.

In summary, we have presented the absorption cross sec-

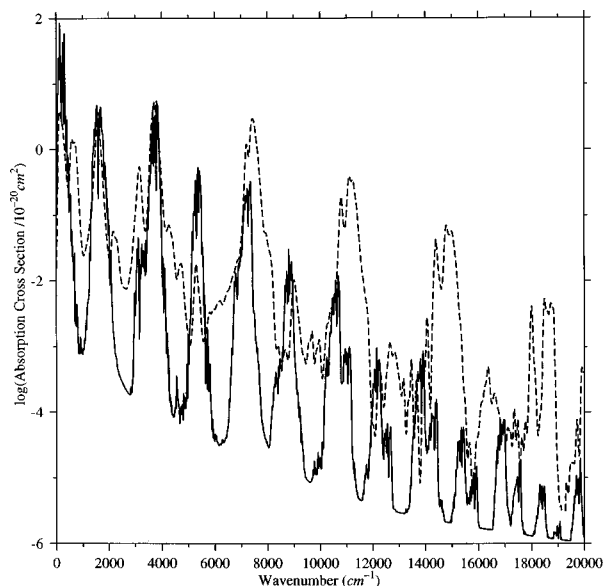


FIG. 4. Logarithm of two times the measured absorption cross section (solid curves) of water vapor averaged within 10 cm^{-1} taken from the experimental and semiempirical HITRAN database at $T=10\text{ }^\circ\text{C}$. For clarity, the high resolution water vapor data have been averaged over windows of width 10 cm^{-1} . The dashed curve is the logarithm of the calculated absorption cross section of water dimer.

tion of the water dimer for frequencies up to $20\,000\text{ cm}^{-1}$. Intermolecular fundamentals are heavily broadened due to the anharmonicity of the intermolecular interaction and the rotation of the dimer. The intramolecular fundamentals are also broadened by mixing with intermolecular excitations and rotation excitations of the dimer. Harmonics beyond 4000 cm^{-1} are quite strong due to the anharmonicity of the O–H bond and the large movement of hydrogen atoms. In comparison, combinations between stretching and bending modes are not as significant. The absorption cross section decreases approximately as an exponential function of frequency.

ACKNOWLEDGMENTS

This work was partially supported by the Atmospheric Environment Service and the Natural Sciences and Engineering Research Council of Canada and by the U.S. Department of Energy.

APPENDIX A

The matrix elements required for the evaluation of angular correlation functions in Eqs. (18) are as follows:

$$\mathcal{R}_{11}(\theta, \phi, \psi) = \cos \psi \cos \phi - \cos \theta \sin \phi \sin \psi, \quad (\text{A1})$$

$$\mathcal{R}_{12}(\theta, \phi, \psi) = -\sin \psi \cos \phi - \cos \theta \sin \phi \cos \psi, \quad (\text{A2})$$

$$\mathcal{R}_{13}(\theta, \phi, \psi) = \sin \theta \sin \phi, \quad (\text{A3})$$

$$\mathcal{R}_{21}(\theta, \phi, \psi) = \cos \psi \sin \phi + \cos \theta \cos \phi \sin \psi, \quad (\text{A4})$$

$$\mathcal{R}_{22}(\theta, \phi, \psi) = -\sin \psi \sin \phi + \cos \theta \cos \phi \cos \psi, \quad (\text{A5})$$

$$\mathcal{R}_{23}(\theta, \phi, \psi) = -\sin \theta \cos \phi, \quad (\text{A6})$$

$$\mathcal{R}_{31}(\theta, \phi, \psi) = \sin \theta \sin \psi, \quad (\text{A7})$$

$$\mathcal{R}_{32}(\theta, \phi, \psi) = \sin \theta \cos \psi, \quad (\text{A8})$$

$$\mathcal{R}_{33}(\theta, \phi, \psi) = \cos \theta. \quad (\text{A9})$$

The coefficients B in Eqs. (27) and (28) are as follows:

$$B_0(x) = 1 - x + \frac{x^2}{4} - \frac{x^3}{12} + \frac{x^4}{144} + \dots, \quad (\text{A10})$$

$$B_1(x) = 1 - \frac{2}{3}x + \frac{1}{6}x^2 - \frac{1}{30}x^3 + \dots, \quad (\text{A11})$$

$$B_2(x) = \frac{1}{4} - \frac{1}{6}x + \frac{1}{36}x^2 + \dots, \quad (\text{A12})$$

$$B_3(x) = \frac{1}{36} - \frac{1}{30}x + \dots, \quad (\text{A13})$$

$$B_4(x) = \frac{1}{144} + \dots. \quad (\text{A14})$$

The coefficients C in Eq. (24) are as follows:

$$C_0 = 1 + \frac{n_+^2}{16R_0^4} + \frac{n_+^4}{64R_0^8} + \frac{n_+^3}{16R_0^6} + \dots, \quad (\text{A15})$$

$$C_1 = 1 + \frac{n_+}{R_0^2} + \frac{n_+^2}{R_0^4} + \frac{11n_+^3}{8R_0^6} + \dots, \quad (\text{A16})$$

$$C_2 = 1 + \frac{2n_+}{R_0^2} + \frac{3n_+^2}{R_0^4} + \dots, \quad (\text{A17})$$

$$C_3 = 2 + \frac{6n_+}{R_0^2} + \dots, \quad (\text{A18})$$

$$C_4 = 4 + \dots, \quad (\text{A19})$$

with $n_+ \equiv N_{\mu_+}^>(0) = N_{\mu_+}^<(0)$. The coordinate of the hydrogen nuclei, oxygen nucleus, and the negative point charge of the RWK2 model in the body-axis frame are as follows:

$$\mathbf{r}_{1\mu} = \left[-R_{1\mu} + \frac{m}{m+M} (R_{1\mu} + R_{2\mu}) \right] \cos\left(\frac{\vartheta_\mu}{2}\right) \hat{\mathbf{e}}_x^\mu + \left[R_{1\mu} - \frac{m}{m+M} (R_{1\mu} - R_{2\mu}) \right] \sin\left(\frac{\vartheta_\mu}{2}\right) \hat{\mathbf{e}}_y^\mu, \quad (\text{A20})$$

$$\mathbf{r}_{2\mu} = \left[-R_{2\mu} + \frac{m}{m+M} (R_{1\mu} + R_{2\mu}) \right] \cos\left(\frac{\vartheta_\mu}{2}\right) \hat{\mathbf{e}}_x^\mu - \left[R_{1\mu} + \frac{m}{m+M} (R_{1\mu} - R_{2\mu}) \right] \sin\left(\frac{\vartheta_\mu}{2}\right) \hat{\mathbf{e}}_y^\mu, \quad (\text{A21})$$

$$\mathbf{r}_{3\mu} = \frac{m}{m+M} (R_{1\mu} + R_{2\mu}) \cos\left(\frac{\vartheta_\mu}{2}\right) \hat{\mathbf{e}}_x^\mu - \frac{m}{m+M} \times (R_{1\mu} - R_{2\mu}) \sin\left(\frac{\vartheta_\mu}{2}\right) \hat{\mathbf{e}}_y^\mu, \quad (\text{A22})$$

$$\mathbf{r}_{4\mu} = \left(-\frac{d}{2R_0 \cos \frac{\vartheta_0}{2}} + \frac{m}{m+M} \right) (R_{1\mu} + R_{2\mu}) \times \cos\left(\frac{\vartheta_\mu}{2}\right) \hat{\mathbf{e}}_x^\mu + \left(\frac{d}{2R_0 \cos \frac{\vartheta_0}{2}} - \frac{m}{m+M} \right) \times (R_{1\mu} - R_{2\mu}) \sin\left(\frac{\vartheta_\mu}{2}\right) \hat{\mathbf{e}}_y^\mu. \quad (\text{A23})$$

Typical matrix elements used to simplify dimer rotation correlation functions in Eq. (18) are as follows:

$$\begin{aligned} \langle r | [R_{11}^D(t_1), R_{11}^D(t_2)] | r \rangle &= \langle r | [R_{21}^D(t_1), R_{21}^D(t_2)] | r \rangle \\ &= \langle r | [R_{12}^D(t_1), R_{12}^D(t_2)] | r \rangle \\ &= \langle r | [R_{22}^D(t_1), R_{22}^D(t_2)] | r \rangle, \end{aligned} \quad (\text{A24})$$

$$\langle r | [R_{23}^D(t_1), R_{23}^D(t_2)] | r \rangle = \langle r | [R_{13}^D(t_1), R_{13}^D(t_2)] | r \rangle, \quad (\text{A25})$$

$$\langle r | [R_{31}^D(t_1), R_{31}^D(t_2)] | r \rangle = \langle r | [R_{32}^D(t_1), R_{32}^D(t_2)] | r \rangle. \quad (\text{A26})$$

APPENDIX B: ROTATION OF THE DIMER

The spectral weight function of rotational excitations of the dimer written in terms of rotational matrix elements is

$$\mathcal{F}_{\text{av}}(\omega) = \sum_r \frac{e^{-\beta E_r}}{\mathcal{Z}} \int_{-\infty}^{\infty} dt e^{i\omega t} \frac{1}{2} \sum_{a,b}^3 (1 + \delta_{a3} \delta_{b3}) \times \langle r | [\mathcal{R}_{ab}^D(t), \mathcal{R}_{ab}^D(0)] | r \rangle, \quad (\text{B1})$$

where $|r\rangle = |\omega_\phi, \omega_\psi\rangle$ and \mathcal{Z} is the partition function. Since $I_a^D \approx I_b^D$, we consider the dimer as an accidentally symmetric top with principal moments of inertia $I_o^D = (I_a^D + I_b^D)/2$ and I_c^D . If we pick the direction of the total angular momentum of the dimer as the z axis of the laboratory frame and the direction of the total angular velocity as the z axis of the body axis, there are two constants of motion such that $\langle r | \dot{\phi}_D^2 | r \rangle = \omega_\phi^2$ and $\langle r | \dot{\psi}_D^2 | r \rangle = \omega_\psi^2$ are constants which are related to the rotational energy E_r by

$$E_r = \frac{I_o^D \omega_\phi^2}{2} + \left(\frac{1}{I_c^D} - \frac{1}{I_o^D} \right) \frac{I_c^D \omega_\psi^2}{2}. \quad (\text{B2})$$

The motion described by its Eulerian angles is a simple harmonic motion and the equations of motion are

$$\begin{aligned} \left(\frac{\partial^2}{\partial t_1^2} + \omega_\phi^2 \right) \langle r | [\mathcal{R}_{23}^D(t_1), \mathcal{R}_{23}^D(t_2)] | r \rangle \\ = -i \frac{\delta(t_1 - t_2)}{2I_o^D} \mathcal{F}_{23}, \end{aligned} \quad (\text{B3})$$

$$\begin{aligned} \left(\frac{\partial^2}{\partial t_1^2} + \omega_\psi^2 \right) \langle r | [\mathcal{R}_{32}^D(t_1), \mathcal{R}_{32}^D(t_2)] | r \rangle \\ = -i \frac{\delta(t_1 - t_2)}{3} \left(\frac{2}{I_c^D} + \frac{1}{I_o^D} \right) \mathcal{F}_{32}, \end{aligned} \quad (\text{B4})$$

$$\frac{\partial}{\partial t_1} \langle r | [\mathcal{R}_{33}^D(t_1), \mathcal{R}_{33}^D(t_2)] | r \rangle = 0, \quad (\text{B5})$$

$$\left[\left(\frac{\partial^2}{\partial t_1^2} + \omega_\phi^2 + \omega_4^2 \right)^2 - 4\omega_\phi^2 \omega_4^2 \right] \langle r | [\mathcal{R}_{11}^D(t_1), \mathcal{R}_{11}^D(t_2)] | r \rangle = -i \frac{\delta(t_1 - t_2)}{6} \left(\frac{2}{I_c^D} + \frac{1}{I_o^D} \right) \mathcal{F}_{11}, \quad (\text{B6})$$

with

$$\omega_4 = \left(\frac{1}{I_c^D} - \frac{1}{I_o^D} \right) I_c^D \omega_\psi, \quad (\text{B7})$$

$$\mathcal{F}_{23} = \langle r | [\mathcal{R}_{23}^D(t_2), \mathcal{R}_{23}^D(t_2)] | r \rangle. \quad (\text{B8})$$

The constants \mathcal{F}_{ij} are obtained from the self-consistent condition such that when t of $\langle R_{ij}^D(t) R_{ij}^D(0) \rangle$ goes to zero, it reduces to the same function of a nonrotating dimer. For instance, after solving Eq. (B3), we obtain

$$\begin{aligned} \mathcal{F}_{23}(\omega) &\equiv \sum_r \frac{e^{-\beta E_r}}{\mathcal{L}} \int dt e^{i\omega t} \langle r | [\mathcal{R}_{23}(t), \mathcal{R}_{23}(0)] | r \rangle \\ &= \sum_r \frac{e^{-\beta E_r}}{\mathcal{L}} \frac{\pi}{2\omega_\phi I_o^D} \mathcal{F}_{23} [\delta(\omega - \omega_\phi) - \delta(\omega + \omega_\phi)]. \end{aligned} \quad (\text{B9})$$

With

$$\lim_{t \rightarrow 0} \langle \mathcal{R}_{23}(t) \mathcal{R}_{23}(0) \rangle = \frac{1}{3} \quad (\text{B10})$$

in the case of a nonrotating dimer, and using Eq. (B9), we found that

$$\begin{aligned} \lim_{t \rightarrow 0} \langle \mathcal{R}_{23}(t) \mathcal{R}_{23}(0) \rangle &= \frac{\mathcal{F}_{23}}{4I_o^D} \sum_r \frac{e^{-\beta E_r}}{\mathcal{L} \omega_\phi} \int_{-\infty}^{\infty} d\omega [\delta(\omega - \omega_\phi) - \delta(\omega + \omega_\phi)] [1 + n(\omega)] \\ &= \frac{\mathcal{F}_{23}}{4I_o^D} \sum_r \frac{e^{-\beta E_r}}{\mathcal{L} \omega_\phi} [1 + 2n(\omega_\phi)] \\ &= \frac{1}{3}. \end{aligned} \quad (\text{B11})$$

There are two frequency scales associated with the above expression, namely $\sqrt{2k_B T / I_o^D}$ and $k_B T / \hbar$. At $T \sim 10^\circ \text{C}$, their ratio, $\sqrt{\hbar^2 2k_B T / (k_B^2 T^2 I_o^D)}$, is about 0.1. The summation is dominated by a narrow range of small ω_ϕ , and therefore, for simplicity, we approximate

$$\mathcal{F}_{23} \approx \frac{4I_o^D \omega_\phi}{3[1 + 2n(\omega_\phi)]} \quad (\text{B12})$$

with the restriction $\omega_\phi < \sqrt{2k_B T / I_o^D}$. In other words,

$$\mathcal{F}_{23}(\omega) \approx \frac{2\pi}{3} \sum_r \frac{e^{-\beta E_r}}{\mathcal{L}} \frac{\delta(\omega - \omega_\phi) - \delta(\omega + \omega_\phi)}{1 + 2n(\omega_\phi)}. \quad (\text{B13})$$

Constants \mathcal{F}_{32} and \mathcal{F}_{11} can be obtained in a similar way. As for the remaining correlation functions, their relationships

are listed in Appendix A. As discussed before, assuming that the energy spectrum E_r is continuous and after the summation is executed, we obtain

$$\begin{aligned} \mathcal{F}_{av}(\omega) &= \frac{2\pi}{1 + 2n(\omega)} \left[\delta(\omega) + \left(\frac{\beta I_o^D}{2\pi} \right)^{\frac{3}{2}} \frac{4\pi}{\beta I_o^D} e^{-\beta I_o^D \omega^2 / 2} \right. \\ &\quad \left. + \left(\frac{\beta I_c^D}{2\pi} \right)^{\frac{3}{2}} \frac{6\pi}{\beta I_c^D} e^{-\beta I_c^D \omega^2 / 2} \right]. \end{aligned} \quad (\text{B14})$$

- ¹R. D. Cess, M. H. Zhang, P. Minnis, L. Corsetti, E. G. Dutton, B. W. Forgan, D. P. Garber, W. L. Gates, J.-J. Morcrette, G. L. Potter, V. Ramanathan, B. Subasilar, C. H. Whitlock, D. F. Young, and Y. Zhou, *Science* **267**, 496 (1995).
- ²V. Ramanathan *et al.*, *Science* **267**, 499 (1995).
- ³P. Pilewskie and F. Valero, *Science* **267**, 1626 (1995).
- ⁴Z. Li, H. W. Barker, and L. Moreau, *Nature (London)* **376**, 486 (1995).
- ⁵Z. Li, L. Moreau, and A. Arking, *Bull. Am. Meteorol. Soc.* **78**, 53 (1997).
- ⁶T. P. Charlock and T. L. Alberta, *Bull. Am. Meteorol. Soc.* **77**, 2673 (1996).
- ⁷A. Arking, *Science* **273**, 779 (1996).
- ⁸J. T. Kiehl, *Phys. Today* **47**, 36 (1994).
- ⁹J. T. Kiehl, J. J. Hack, M. H. Zhang, and R. D. Cess, *J. Clim.* **8**, 2200 (1995).
- ¹⁰J. P. Peixoto and A. H. Oort, *Physics of Climate* (AIP, New York, 1992).
- ¹¹P. Chýlek and D. J. W. Geldart, *Geophys. Res. Lett.* **24**, 2015 (1997).
- ¹²P. Chýlek, Q. Fu, H. C. W. Tso, and D. J. W. Geldart (unpublished).
- ¹³Z. Slanina, *J. Atmos. Chem.* **6**, 185 (1988).
- ¹⁴D. F. Coker, R. E. Miller, and R. O. Watts, *J. Chem. Phys.* **82**, 3554 (1985).
- ¹⁵J. R. Reimers and R. O. Watts, *Mol. Phys.* **52**, 357 (1984).
- ¹⁶J. R. Reimers and R. O. Watts, *Chem. Phys.* **85**, 83 (1984).
- ¹⁷J. R. Reimers, R. O. Watts, and L. M. Klein, *Chem. Phys.* **64**, 95 (1982).
- ¹⁸D. F. Coker, J. R. Reimers, and R. O. Watts, *Aust. J. Phys.* **35**, 623 (1982).
- ¹⁹D. F. Coker and R. O. Watts, *J. Phys. Chem.* **91**, 2513 (1987).
- ²⁰M. Munoz-Caro and A. Nino, *J. Phys. Chem. A* **101**, 4128 (1997).
- ²¹K. S. Kim, B. J. Mhin, U. S. Choi, and K. Lee, *J. Chem. Phys.* **97**, 6649 (1992).
- ²²M. Van Thiel, E. D. Becker, and G. C. Pimentel, *J. Chem. Phys.* **27**, 486 (1957).
- ²³T. R. Dyke, K. M. Mack, and J. S. Muentzer, *J. Chem. Phys.* **66**, 498 (1977).
- ²⁴R. M. Bentwood, A. J. Barnes, and W. J. Orville-Thomas, *J. Mol. Spectrosc.* **84**, 391 (1980).
- ²⁵M. F. Vernon, D. J. Krajnovich, K. S. Kwok, J. M. Lisy, Y. R. Shen, and Y. T. Lee, *J. Chem. Phys.* **77**, 47 (1982).
- ²⁶S. H. Suck, A. E. Wetmore, T. S. Chen, and J. L. Kassner, *Appl. Opt.* **21**, 1610 (1982).
- ²⁷R. P. Page, J. G. Frey, Y. R. Shen, and Y. T. Lee, *Chem. Phys. Lett.* **106**, 373 (1984).
- ²⁸F. Huisken, M. Kaloudis, and A. Kulcke, *J. Chem. Phys.* **104**, 17 (1996).
- ²⁹G. Herzberg, *Molecular Spectra and Molecular Structure III*, 2nd ed (Krieger, Malabar, 1966).
- ³⁰W. S. Struve, *Fundamentals of Molecular Spectroscopy* (Wiley, New York, 1989).
- ³¹A. L. Fetter and J. D. Walecka, *Quantum Theory of Many-Particle Systems* (McGraw-Hill, New York, 1971).
- ³²T. R. Koehler, *Dynamical Properties of Solids*, edited by G. K. Horton and A. A. Maradudin (North-Holland, Oxford 1975), Vol. 2.
- ³³H. Horner, *Z. Phys.* **242**, 432 (1971).
- ³⁴H. Horner, *Low Temperature Physics-LT 13*, edited by K. D. Timmerhaus, W. J. O'Sullivan, and E. F. Hammel (Plenum, New York, 1972).
- ³⁵H. Horner, *Computational Solid State Physics*, edited by F. Herman, N. W. Dalton, and T. R. Koehler (Plenum, New York 1972).
- ³⁶L. S. Rothman *et al.*, *J. Quant. Spectrosc. Radiat. Transf.* **48**, 469 (1992).
- ³⁷L. S. Rothman, R. R. Gamache, A. Goldman, L. R. Brown, R. A. Toth, H. M. Pickett, R. L. Poynter, J.-M. Flaud, C. Camy-Peyret, A. Barbe, N. Husson, C. P. Rinsland, and M. A. H. Smith, *Appl. Opt.* **7**, 469 (1992).